Integrated Bioinformatics Analysis Identifies Pyroptosis-related Genes in Alzheimer's Disease

Tong Guo (guotong@ccmu.edu.cn)
Capital Medical University

YuFen Wang
The Second Affiliated Hospital of Henan University of Traditional Chinese Medicine

Research Article

Keywords: Alzheimer's disease, pyroptosis, CASP6, neuroinflammation

Posted Date: February 2nd, 2022

DOI: https://doi.org/10.21203/rs.3.rs-1310823/v1

Abstract

Background: Recent studies have shown the association between Alzheimer's disease (AD) and inflammation. Pyroptosis is an inflammatory type of programmed cell death, and it has been associated with AD. Herein, we aimed to explore the potential role of pyroptosis-related genes in AD, advancing the understanding of pyroptosis-related genes in AD pathogenesis.

Methods: Based on the gene expression profile in GSE5281, we screened for differentially expressed genes (DEGs), performed a weighted gene correlation analysis (WGCNA), and identified the most AD-related module. After intersecting the hub genes in this module with 52 pyroptosis-related genes, we obtained the key genes to construct a least absolute shrinkage and selection operator (LASSO) model for AD. We also constructed a CASP6-focused interaction network including several hub genes. The LASSO model and expression of CASP6 were evaluated in GSE122063 and GSE132903.

Results: Through WGCNA, four functional modules were identified, of which the brown module is most significantly related to AD (correlation coefficient=0.93, P=4e-13). CASP6 is aberrantly highly expressed in AD and closely connected with hub genes in the brown module. Seven genes (CASP6, BAK1, CASP5, CHMP4B, CHMP4C, IRF2, PLCG1) were identified as key genes, and the LASSO model based on key genes can predict AD with medium-to-high accuracy in train, test and validation set (AUC=0.898, 0.811, 0.857, respectively).

Conclusions: Highly expressed CASP6 interact with other pyroptosis-related genes in AD, shedding light on the potential role of pyroptosis in AD pathogenesis.

Introduction

Alzheimer's disease (AD) is the most common neurodegenerative disease worldwide, the incidence and prevalence of which are expected to increase as the aging process of population accelerates[1, 2]. However, as a multifactorial and complex disease, the exact pathogenesis of AD remains unclear, thus there being no effective therapeutic strategy to cure the disease[3]. Molecular features include senile plaques consisting of depositing amyloid beta peptides (Aβ), neurofibrillary tangles consisting of hyperphosphorylated tau protein[4, 5]. Recent studies revealed elevated levels of pro-inflammatory cytokines may contribute to AD, suggesting AD as a systematic inflammatory disease[6-8].

Pyroptosis is an inflammatory type of programmed cell death, characterized by caspases activation, gasdermin D (GSDMD) cleavage and pro-inflammatory mediators release[9, 10]. Studies have shown the potential relationship between pyroptosis and AD[11]. For example, caspase-6 (CASP6) plays a key role in pyroptosis.As a member of caspase family, CASP6 is categorized as an executioner but shows some differences the other executioners, aberrantly activated at the early stage of AD[12]. Studies have shown that high expression of CASP6 is related to anxiety behavior and worse memory in AD mice[13].

However, the role of pyroptosis-related genes in AD remains unclear. Herein, we conducted systematic bioinformatics analyses to investigate the expression trait of pyroptosis-related genes in AD and construct a LASSO model for AD based on genes related to both pyroptosis and AD, possibly suggesting the pathogenesis of AD from pyroptotic perspective.

Results

Identification of DEGs

A total of 3341 differentially expressed genes (DEGs) were identified in AD patients compared to healthy controls, of which 1878 were upregulated and 1463 were downregulated (**Figure 2A**). The top 25 upregulated and downregulated DEGs were visualized in a heatmap (**Figure 2B**).

WGCNA and Analysis of the most AD-Associated Module

Through weighted gene correlation analysis(WGCNA) based on 3341 DEGs identified in AD and control samples, we identified four modules in total (**Figure 3A**), of which the brown module is most significantly related to AD (correlation coefficient=0.93, P=4e-13; **Figure 3B**) and was defined as the candidate module of interest. To further analyze this module, we conducted functional enrichment analyses, which were shown in **Figure 4**. According to Gene Ontology (GO) analysis, genes in the brown module are significantly enriched in the immune responses to antigens and the processes of cell proliferation and homeostasis (**Figure 4A and 4B**). Moreover, Kyoto Encyclopedia of Genes and Genomes (KEGG) analysis indicated that brown module genes are involved in the signaling pathways related to cell death, apoptosis and inflammation as well as the development of many neurodegenerative diseases, including AD (**Figure 4C and 4D**).

Identification of Key Genes

According to screening criteria of gene significance(GS)> 0.8 and module membership (MM)> 0.85, 190 hub genes were identified from the brown module. After intersecting them with pyroptosis-related genes, we finally obtained seven key genes (CASP6, BAK1, CASP5, CHMP4B, CHMP4C, IRF2, PLCG1) for the construction of predictive model for AD (**Figure 5A**). As shown in **Figure 5B**, there was a connection between the expression levels of these key genes, indicating the potential interaction among them. By referring to the literature, we focused on CASP6 to further explore the association between pyroptosis and AD[12, 13]. There were 149 DEGs screened in CASP6-high samples compared to CASP6-low samples, consisting of 92 upregulated genes and 57 downregulated ones (**Figure 5C**). Moreover, we uncovered 135 overlapping genes after crossing themwith DEGsidentified in AD patients compared to healthy controls (**Figure 5D**), indicating some DEGs related to the expression of CASP6 are also associated with AD.

Validation of CASP6 Expression and Construction of CASP6-focused Interaction Network

To validate the expression level of CASP6 in AD patients and healthy controls, we investigated the expression profile of CASP6 in GSE122063 (**Figure 6B**) and GSE132903 (**Figure 6C**), noticing that, similar to the trend in GSE5281 (**Figure 6A**), CASP6 was significantly upregulated in AD patients than healthy controls (all P <0.001), which indicated the association between CASP6 and AD[18]. Furthermore, we constructed the CASP6-focused interaction network based on the hub genes interacted with CASP6 (**Figure 7A and 7B**). Functional enrichment analyses showed that these genes were significantly involved in apoptosis, development and homeostasis of neurons (**Figure 7C and 7D**), suggesting the potential role of CASP6 in AD, possibly by interacting with these hub genes.

Construction and Validation of predictive LASSO model

We selected the seven key genes associated with both AD and pyroptosis to construct a least absolute shrinkage and selection operator (LASSO) model for AD (**Figure 8A**). Finally, with the maximum of area under the curve(AUC) as 0.898 (**Figure 8B**), five genes were included in the model formula with non-zero coefficients, which were listed in Table 1. According to receiver operating characteristic (ROC) analyses, the AUC value of this model was 0.811 in the test set (**Figure 8C**) and 0.857 in the validation set (**Figure 8D**), suggesting our pyroptosis-related LASSO model as a predictive biomarker for AD.

Table1. Five pyroptosis-related genes included in the LASSO model for AD.

Gene	Coefficient
CASP6	1.47826822842227
PLCG1	0.844799998060399
IRF2	0.0605103126266471
CASP5	-0.19850370527142
CHMP4B	-0.407690009907354
(Intercept)	-12.0503859698135

Discussion

AD is the most common neurodegenerative disease, the incidence and prevalence of which are expected to increase as the aging process of population accelerates[1, 2]. Emerging studies have shown excessive inflammatory activation as well as pyroptosis, the inflammation-associated programmed cell death, contributes to neurodegenerative diseases including AD[11]. Therefore, we further investigated the underlying role of pyroptosis-related genes in AD by bioinformatic analyses.

First, we screened for DEGs in based on the difference in the state of disease, the results of which are similar to related studies[19, 20]. Conducting WGCNA, we identified the module most significantly related to AD, and obtained 190 potential hub genes according to GS > 0.8 and MM > 0.85. After intersecting hub genes with pyroptosis-related genes, we finally identified seven closely connected key genes, including CASP6, BAK1, CASP5, CHMP4B, CHMP4C, IRF2, PLCG1.

We further extracted the expression profile of these key genes to construct a LASSO model, which contains five genes (CASP6, CASP5, CHMP4B, IRF2 and PLCG1) with non-zero coefficients. CASP6 has been linked to pyroptosis, serving as a crucial enhancer of the pyroptotic pathway[21-23]. We identified DEGs according to the expression level of CASP6, finding there are overlapping DEGs identified from different CASP6 levels and AD. In addition, we investigated and verified the expression trait of CASP6 in three datasets, finding that CASP6 is consistently upregulated in AD patients compared to healthy controls, which indicates that high expression of CASP6 may contribute to the development of AD. This is consistent with previous studies[13, 24, 25]. Angel et al. [13]found that compared to controls, CASP6-knocked-out AD mice had a significant decrease in Aβ and proinflammatory cytokines TNF-α, together with ameliorated microglia activity and improved AD symptoms, which indicates CASP6 may contribute to AD through inflammation. Similarly, Klaiman et al.[25]also found that neuritic activation of CASP6 may disrupt the neural cytoskeleton network and normal function, aggravating neurodegeneration. Additionally, the CASP6-focused interaction network based on seven hub genes suggests that CASP6 interacts with genes involved in the development and homeostasis of nervous system, which further supports the potential role of CASP6 in AD, possibly by interacting with hub genes.

Apart from CASP6, some of the other pyroptosis-related genes have been linked to AD. For instance, phospholipase Cγ1 (PLCG1) plays a key role in intracellular signal transduction[26] and is involved in several neurological disorders[27-31]. In AD, PLCG1 was significantly reduced[32],and possible mechanisms are mainly based on the tau hypothesis[33]. Tangled tau disrupts the normal function of neurons, contributing to memory loss and other symptoms of AD[34, 35]. PLCG1 binds to tau via its SH3 domain, indicating its indirect association with AD[36, 37]. More recently, Kim et al.[38]found single -nucleotide variations of AD mice were mainly distributed in the PLCG1 gene body, further suggesting the potential of PLCG1 in AD. Interferon regulatory factor 2 (IRF2) regulates the interferon system along with TRIM22 and STAT1[39, 40]. According to Ahmed et al.[41], SARS-CoV-2-induced exosomes contain several transcriptional factors, including IRF2, which may dysregulate the gene network of neurons, attenuating neurodegeneration. What's more, IRF2 also regulates CASP4 levels and activates GSDMD, facilitating cytosolic LPS-mediated pyroptosis[42, 43]. This indicates the possible pyroptotic mechanism of IRF2 in AD. The LASSO model we constructed may serve as a biomarker of AD, and the five pyroptosis-related genes included shed light on the potential mechanisms of AD from the pyroptosis perspective.

Functional enrichment analyses showed that the most significantly AD-related module highly involved in the biological processes linked to immune responses to antigens, cell proliferation and homeostasis, and in the signaling pathways related to cell death, apoptosis, inflammation and many neurodegenerative

diseases including AD. As members of programmed cell death, pyroptosis and apoptosis were identified with crosstalk and co-regulation pathways[44, 45]. Zheng et al.[21-23] raised the term PANoptosis (a combination of pyroptosis, apoptosis and necroptosis), indicating these types of cell death is coordinated and co-regulated by a multiprotein complex named PANoptosome, which contains RIPK3, ZBP1 and NLRP3 inflammasome. CASP6 can bind to RIPK3, enhancing the interaction between RIPK3 and ZBP1, facilitating the formation of ZBP1-NLRP3 inflammasome and the process of PANoptosis significantly[21-23]. Taking together the signaling pathways enriched in CASP6-focused interaction network, our data suggested the potential pyroptosis-related pathogenesis of AD.

Our study suggested the underlying mechanisms of pyroptosis in AD by identifying key molecules and constructing LASSO model related to pyroptosis. However, in vivo and in vitro experiments are required to further confirm the potential key genes and pathways.

Conclusions

Collectively, CASP6 and six other pyroptosis-related genes may be involved in the development of AD. A five-gene LASSO model, including CASP6, CASP5, CHMP4B, IRF2 and PLCG1, may serve as a biomarker for AD. Our data suggested the underlying mechanism of AD from the pyroptotic perspective.

Materials And Methods

Data Acquisition

Three datasets (GSE5281, GSE122063 and GSE132903), which contain the gene expression profile of AD patients and healthy controls, were downloaded from the Gene Expression Omnibus (GEO) database (https://www.ncbi.nlm.nih.gov/geo/) to conduct the following processes illustrated in **Figure 1**. GSE5281, including 87 AD patients and 74 healthy controls' brain tissue samples, was used to explore the potential role of CASP6 and other pyroptosis genes in AD. GSE122063 contains the gene expression of 56 AD patients and 44 healthy controls, and GSE132903 includes the gene expression of 97 AD patients and 98 healthy controls, which were both used for the verification of the pyroptosis-gene-based model as well as the differential expression of CASP6 in AD.

Screening for DEGs in AD

Using the R package "limma"[14], we screened the DEGs (adjusted $P<0.05$ and $|\log2 \text{ fold change (FC)}| \geq 1$) between AD and control, as well as between CASP6-high and CASP6-low in GSE5281. The median expression level of CASP6 was defined as the cutoff point.

Construction of Co-Expression Network

By the R package "WGCNA"[15], we constructed the co-expression network of the DEGs in GSE5281. The soft-threshold power value was calculated during the process by the pickSoftThreshold function.

Candidate power ranged from 1 to 20, and we chose the power value when the correlation coefficient threshold reached 0.9. The cut height threshold was defined as 0.2 for the merging of similar modules. We finally chose the module with the highest correlation coefficient, which is most associated to AD, for further analysis.

Functional Enrichment Analysis

Utilizing the R package “clusterprofiler”[16], we conducted GO and KEGG analyses to further explore the significant (P<0.05) pathways of DEGs in the most AD-related module. The R packages “ggplot2” and “enrichplot” were used to visualize the top 10 terms of molecular functions, cellular components and biological processes.

Identification of Key Genes

DEGs in the candidate module with GS>0.8 andMM>0.85 were considered as hub genes. By searching the published literature, we collected 52 pyroptosis-related genes (listed in the Supplementary Table). After intersecting them with the hub genes, we finally uncovered the key genes of interest. The R package “corrplot” was used to visualize the correlation among these key genes.

Validation of CASP6 Expression and Construction of CASP6-focused Interaction Network

Expression level of CASP6 was evaluated in GSE5281, GSE122063 and GSE132903. The comparison result was visualized with the R package “ggpubr”. In addition, we explored the hub genes which interact with CASP6 (confidence score>0.7) using the STRING database (https://string-db.org)[17] and visualized the interactions using Cytoscape3.9.0 software. We also performed functional enrichment analyses for CASP6 and its interacted hub genes by the R package “clusterprofiler”[16].

Construction and Validation of a LASSO Model

In order to explore the potential correlation between the pyroptosis-related key genes selected and AD, a LASSO model was constructed with the R package “glmnet” (https://CRAN.R-project.org/package=glmnet). Considering GSE5281 as the train set, we obtained the coefficients to weight the key genes included in the formula and then tested this model in GSE132903. In addition, GSE122603 was utilized for further validation. With the R package “pROC”, we plotted the ROC curves and calculated the values of AUC to evaluate the LASSO model aiming to distinguish AD patients to healthy controls.

Abbreviations

AD: Alzheimer’s disease

DEG: differentially expressed gene

WGCNA: weighted gene correlation analysis

LASSO: least absolute shrinkage and selection operator

GSDMD: gasdermin D

CASP6: caspase-6

GO: Gene Ontology

KEGG:Kyoto Encyclopedia of Genes and Genomes

GS:gene significance

MM:module membership

AUC:area under the curve

ROC:receiver operating characteristic

PLCG1: phospholipase Cγ1

GEO: Gene Expression Omnibus

Declarations

Ethics approval and consent to participate

GEO belongs to public databases. The patients involved in the database have obtained ethical approval. Users can download relevant data for free for research and publication. Our study is based on open-source data, so there are no ethical issues and other conflicts of interest.

Consent for publication

Not applicable.

Availability of data and materials

Our study is based on open-source data downloaded from GEO database. We included three datasets (GSE5281, GSE122063, GSE132903), which can be found via https://www.ncbi.nlm.nih.gov/geo/query/acc.cgi?acc=GSE5281, https://www.ncbi.nlm.nih.gov/geo/query/acc.cgi?acc=GSE122063, https://www.ncbi.nlm.nih.gov/geo/query/acc.cgi?acc=GSE132903, respectively.

Competing interests

None.

Funding

None.

Authors’ contributions

GT analyzed the data and was a major contributor in writing the manuscript. WYF revised the manuscript and supervised the whole process. All authors read and approved the final manuscript.

Acknowledgements

We acknowledge GEO database for providing their platforms and contributes for uploading their meaningful datasets.

References

[1] Scheltens P, Blennow K, Breteler M M, et al. Alzheimer's disease[J]. Lancet, 2016, 388(10043): 505-17.

[2] Ballard C, Gauthier S, Corbett A, et al. Alzheimer's disease[J]. Lancet, 2011, 377(9770): 1019-31.

[3] Mondragón-Rodríguez S, Basurto-Islas G, Lee H G, et al. Causes versus effects: the increasing complexities of Alzheimer's disease pathogenesis[J]. Expert Rev Neurother, 2010, 10(5): 683-91.

[4] Sun X, Chen W D, Wang Y D. β-Amyloid: the key peptide in the pathogenesis of Alzheimer's disease[J]. Front Pharmacol, 2015, 6: 221.

[5] Hanger D P, Lau D H, Phillips E C, et al. Intracellular and extracellular roles for tau in neurodegenerative disease[J]. J Alzheimers Dis, 2014, 40 Suppl 1: S37-45.

[6] Chen Y, Fang L, Chen S, et al. Gut Microbiome Alterations Precede Cerebral Amyloidosis and Microglial Pathology in a Mouse Model of Alzheimer's Disease[J]. Biomed Res Int, 2020, 2020: 8456596.

[7] Martinez F O, Helming L, Gordon S. Alternative activation of macrophages: an immunologic functional perspective[J]. Annu Rev Immunol, 2009, 27: 451-83.

[8] Agostini A, Yuchun D, Li B, et al. Sex-specific hippocampal metabolic signatures at the onset of systemic inflammation with lipopolysaccharide in the APPswe/PS1dE9 mouse model of Alzheimer's disease[J]. Brain Behav Immun, 2020, 83: 87-111.

[9] Bergsbaken T, Fink S L, Cookson B T. Pyroptosis: host cell death and inflammation[J]. Nat Rev Microbiol, 2009, 7(2): 99-109.

[10] Shi J, Zhao Y, Wang Y, et al. Inflammatory caspases are innate immune receptors for intracellular LPS[J]. Nature, 2014, 514(7521): 187-92.

[11] Voet S, Srinivasan S, Lamkanfi M, et al. Inflammasomes in neuroinflammatory and neurodegenerative diseases[J]. EMBO Mol Med, 2019, 11(6):

[12] De Calignon A, Fox L M, Pitstick R, et al. Caspase activation precedes and leads to tangles[J]. Nature, 2010, 464(7292): 1201-4.

[13] Angel A, Volkman R, Royal T G, et al. Caspase-6 Knockout in the 5xFAD Model of Alzheimer's Disease Reveals Favorable Outcome on Memory and Neurological Hallmarks[J]. Int J Mol Sci, 2020, 21(3):

[14] Ritchie M E, Phipson B, Wu D, et al. limma powers differential expression analyses for RNA-sequencing and microarray studies[J]. Nucleic Acids Res, 2015, 43(7): e47.

[15] Langfelder P, Horvath S. WGCNA: an R package for weighted correlation network analysis[J]. BMC Bioinformatics, 2008, 9: 559.

[16] Yu G, Wang L G, Han Y, et al. clusterProfiler: an R package for comparing biological themes among gene clusters[J]. Omics, 2012, 16(5): 284-7.

[17] Szklarczyk D, Franceschini A, Wyder S, et al. STRING v10: protein-protein interaction networks, integrated over the tree of life[J]. Nucleic Acids Res, 2015, 43(Database issue): D447-52.

[18] Tubeleviciute-Aydin A, Beautrait A, Lynham J, et al. Identification of Allosteric Inhibitors against Active Caspase-6[J]. Sci Rep, 2019, 9(1): 5504.

[19] Rangaraju S, Dammer E B, Raza S A, et al. Identification and therapeutic modulation of a pro-inflammatory subset of disease-associated-microglia in Alzheimer's disease[J]. Mol Neurodegener, 2018, 13(1): 24.

[20] Zou D, Li R, Huang X, et al. Identification of molecular correlations of RBM8A with autophagy in Alzheimer's disease[J]. Aging (Albany NY), 2019, 11(23): 11673-11685.

[21] Zheng M, Kanneganti T D. The regulation of the ZBP1-NLRP3 inflammasome and its implications in pyroptosis, apoptosis, and necroptosis (PANoptosis)[J]. Immunol Rev, 2020, 297(1): 26-38.

[22] Zheng M, Kanneganti T D. Newly Identified Function of Caspase-6 in ZBP1-mediated Innate Immune Responses, NLRP3 Inflammasome Activation, PANoptosis, and Host Defense[J]. J Cell Immunol, 2020, 2(6): 341-347.

[23] Zheng M, Karki R, Vogel P, et al. Caspase-6 Is a Key Regulator of Innate Immunity, Inflammasome Activation, and Host Defense[J]. Cell, 2020, 181(3): 674-687.e13.

[24] Halawani D, Tessier S, Anzellotti D, et al. Identification of Caspase-6-mediated processing of the valosin containing protein (p97) in Alzheimer's disease: a novel link to dysfunction in ubiquitin proteasome system-mediated protein degradation[J]. J Neurosci, 2010, 30(17): 6132-42.

[25] Klaiman G, Petzke T L, Hammond J, et al. Targets of caspase-6 activity in human neurons and Alzheimer disease[J]. Mol Cell Proteomics, 2008, 7(8): 1541-55.

[26] Yang Y R, Choi J H, Chang J S, et al. Diverse cellular and physiological roles of phospholipase C-γ1[J]. Adv Biol Regul, 2012, 52(1): 138-51.

[27] Giralt A, Rodrigo T, Martín E D, et al. Brain-derived neurotrophic factor modulates the severity of cognitive alterations induced by mutant huntingtin: involvement of phospholipaseCgamma activity and glutamate receptor expression[J]. Neuroscience, 2009, 158(4): 1234-50.

[28] He X P, Pan E, Sciarretta C, et al. Disruption of TrkB-mediated phospholipase Cgamma signaling inhibits limbic epileptogenesis[J]. J Neurosci, 2010, 30(18): 6188-96.

[29] Kim D, Jun K S, Lee S B, et al. Phospholipase C isozymes selectively couple to specific neurotransmitter receptors[J]. Nature, 1997, 389(6648): 290-3.

[30] Jang H J, Yang Y R, Kim J K, et al. Phospholipase C-γ1 involved in brain disorders[J]. Adv Biol Regul, 2013, 53(1): 51-62.

[31] Yang Y R, Jung J H, Kim S J, et al. Forebrain-specific ablation of phospholipase Cγ1 causes manic-like behavior[J]. Mol Psychiatry, 2017, 22(10): 1473-1482.

[32] Shimohama S, Matsushima H, Fujimoto S, et al. Differential involvement of phospholipase C isozymes in Alzheimer's disease[J]. Gerontology, 1995, 41 Suppl 1: 13-9.

[33] Yang Y R, Kang D S, Lee C, et al. Primary phospholipase C and brain disorders[J]. Adv Biol Regul, 2016, 61: 80-5.

[34] Querfurth H W, Laferla F M. Alzheimer's disease[J]. N Engl J Med, 2010, 362(4): 329-44.

[35] Aleong R, Aumont N, Dea D, et al. Non-steroidal anti-inflammatory drugs mediate increased in vitro glial expression of apolipoprotein E protein[J]. Eur J Neurosci, 2003, 18(6): 1428-38.

[36] Jenkins S M, Johnson G V. Tau complexes with phospholipase C-gamma in situ[J]. Neuroreport, 1998, 9(1): 67-71.

[37] Reynolds C H, Garwood C J, Wray S, et al. Phosphorylation regulates tau interactions with Src homology 3 domains of phosphatidylinositol 3-kinase, phospholipase Cgamma1, Grb2, and Src family kinases[J]. J Biol Chem, 2008, 283(26): 18177-86.

[38] Kim S H, Yang S, Lim K H, et al. Prediction of Alzheimer's disease-specific phospholipase c gamma-1 SNV by deep learning-based approach for high-throughput screening[J]. Proc Natl Acad Sci U S A, 2021, 118(3):

[39] Gao B, Wang Y, Xu W, et al. A 5' extended IFN-stimulating response element is crucial for IFN-gamma-induced tripartite motif 22 expression via interaction with IFN regulatory factor-1[J]. J Immunol, 2010, 185(4): 2314-23.

[40] Rauch I, Rosebrock F, Hainzl E, et al. Noncanonical Effects of IRF9 in Intestinal Inflammation: More than Type I and Type III Interferons[J]. Mol Cell Biol, 2015, 35(13): 2332-43.

[41] Ahmed S, Paramasivam P, Kamath M, et al. Genetic Exchange of Lung-Derived Exosome to Brain Causing Neuronal Changes on COVID-19 Infection[J]. Mol Neurobiol, 2021, 58(10): 5356-5368.

[42] Benaoudia S, Martin A, Puig Gamez M, et al. A genome-wide screen identifies IRF2 as a key regulator of caspase-4 in human cells[J]. EMBO Rep, 2019, 20(9): e48235.

[43] Kayagaki N, Lee B L, Stowe I B, et al. IRF2 transcriptionally induces GSDMD expression for pyroptosis[J]. Sci Signal, 2019, 12(582):

[44] Lamkanfi M, Kanneganti T D, Van Damme P, et al. Targeted peptidecentric proteomics reveals caspase-7 as a substrate of the caspase-1 inflammasomes[J]. Mol Cell Proteomics, 2008, 7(12): 2350-63.

[45] Malireddi R K, Ippagunta S, Lamkanfi M, et al. Cutting edge: proteolytic inactivation of poly(ADP-ribose) polymerase 1 by the Nlrp3 and Nlrc4 inflammasomes[J]. J Immunol, 2010, 185(6): 3127-30.

Figures

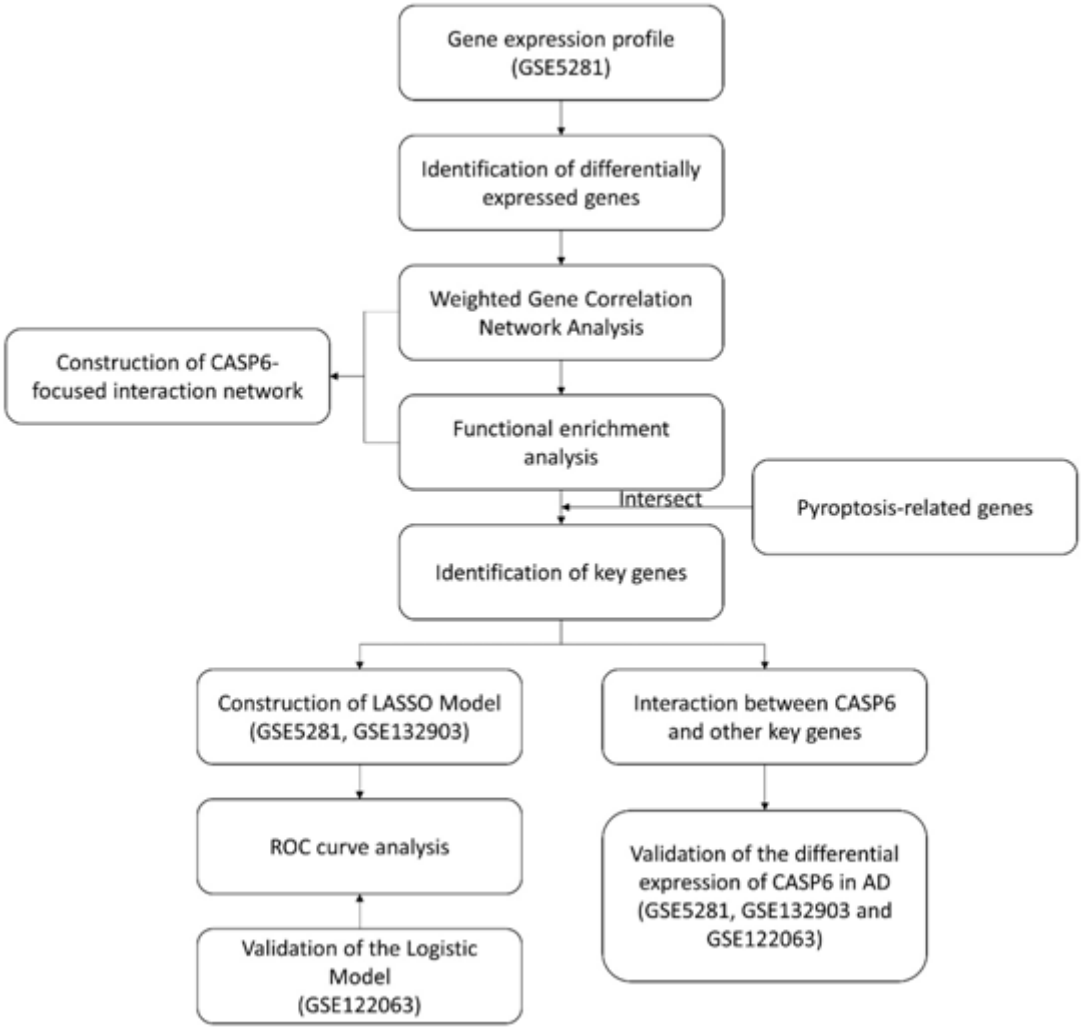

Figure 1

Workflow of the present study.

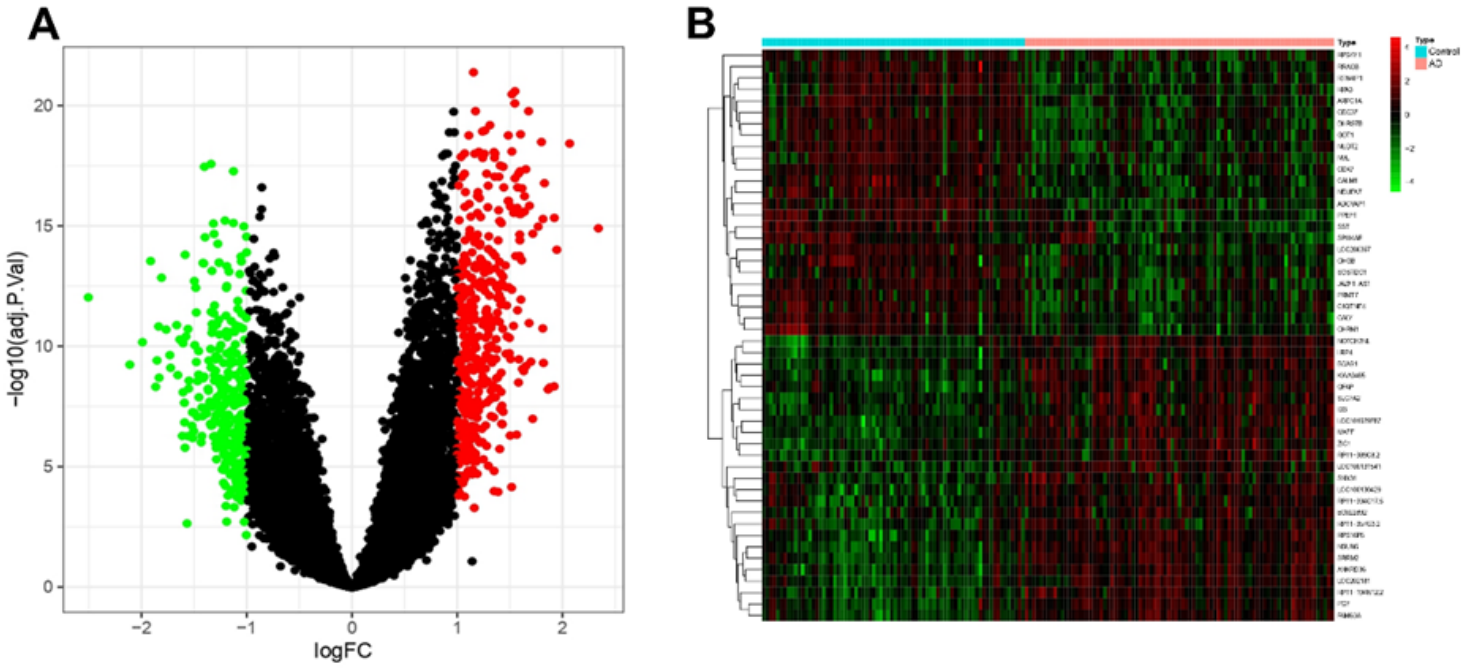

Figure 2

Differentially expressed genes (DEGs) analysis. (**A**) Volcano plot of AD VS control, red represents up-regulated genes, green represents down-regulated genes, and black represents insignificantly differentially expressed genes. (**B**) Heatmap of 25 most up-regulated and 25 most down-regulated genes.

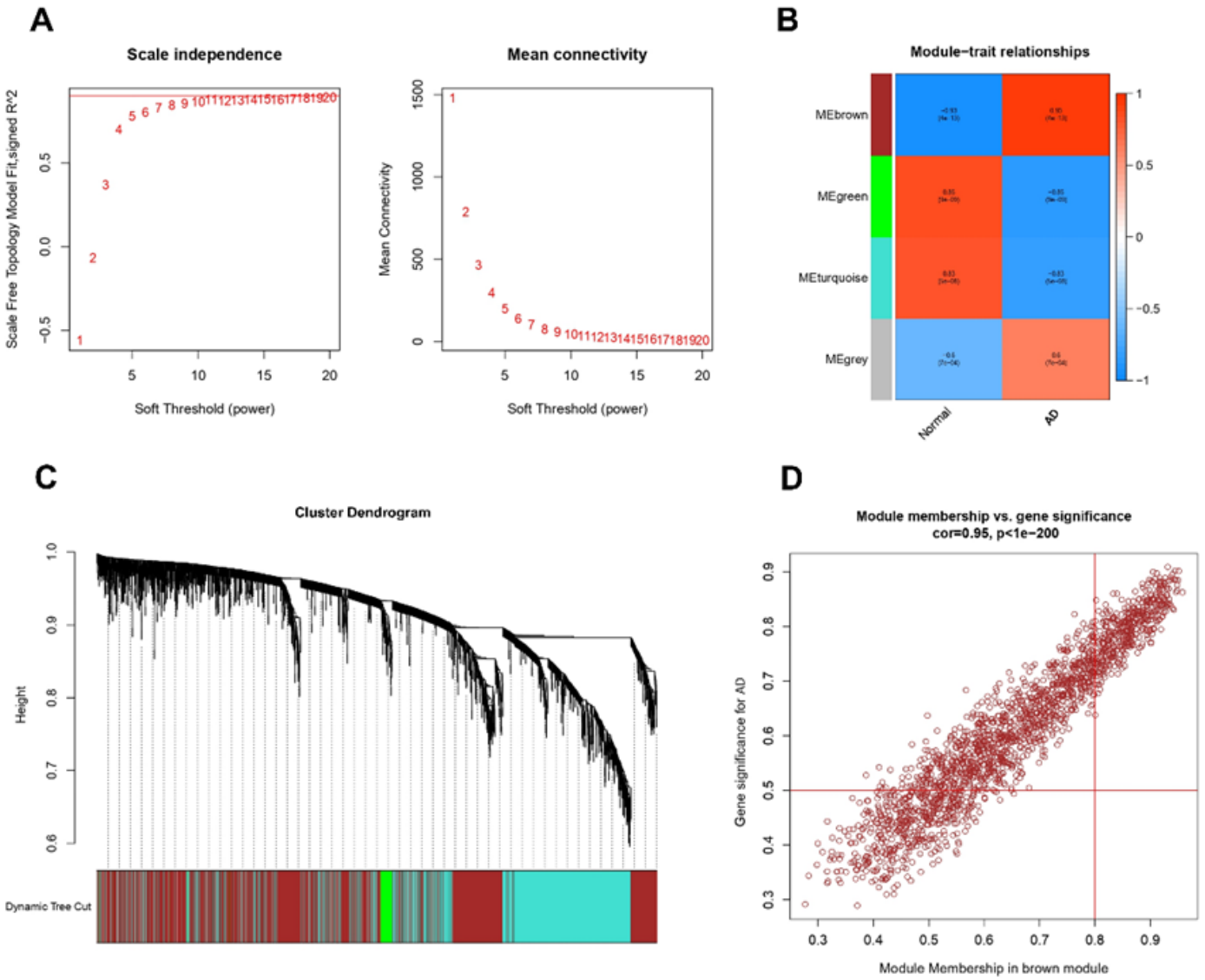

Figure 3

Weighted gene correlation analysis. (**A**) Analysis of the scale-free fit index (Left) and mean connectivity (Right) for candidate soft threshold powers. (**B**) Heatmap of the correlation between modules and AD. Each cell contained the correlation coefficient and corresponding P value. (**C**) Clustering dendrogram of DEGs related to AD. (**D**) Scatter plot of genes in brown module.

Figure 4

Functional enrichment analysis of DEGs in the brown module. (**A**) Bar chart of the top 30 enriched GO annotations, ordered by P value. (**B**) Bubble chart of the top 30 enriched GO annotations, ordered by count of genes. (**C**) Bar chart of the top 30 enriched KEGG pathways, ordered by P value. (**D**) Bubble chart of the top 30 enriched KEGG pathways, ordered by count of genes.

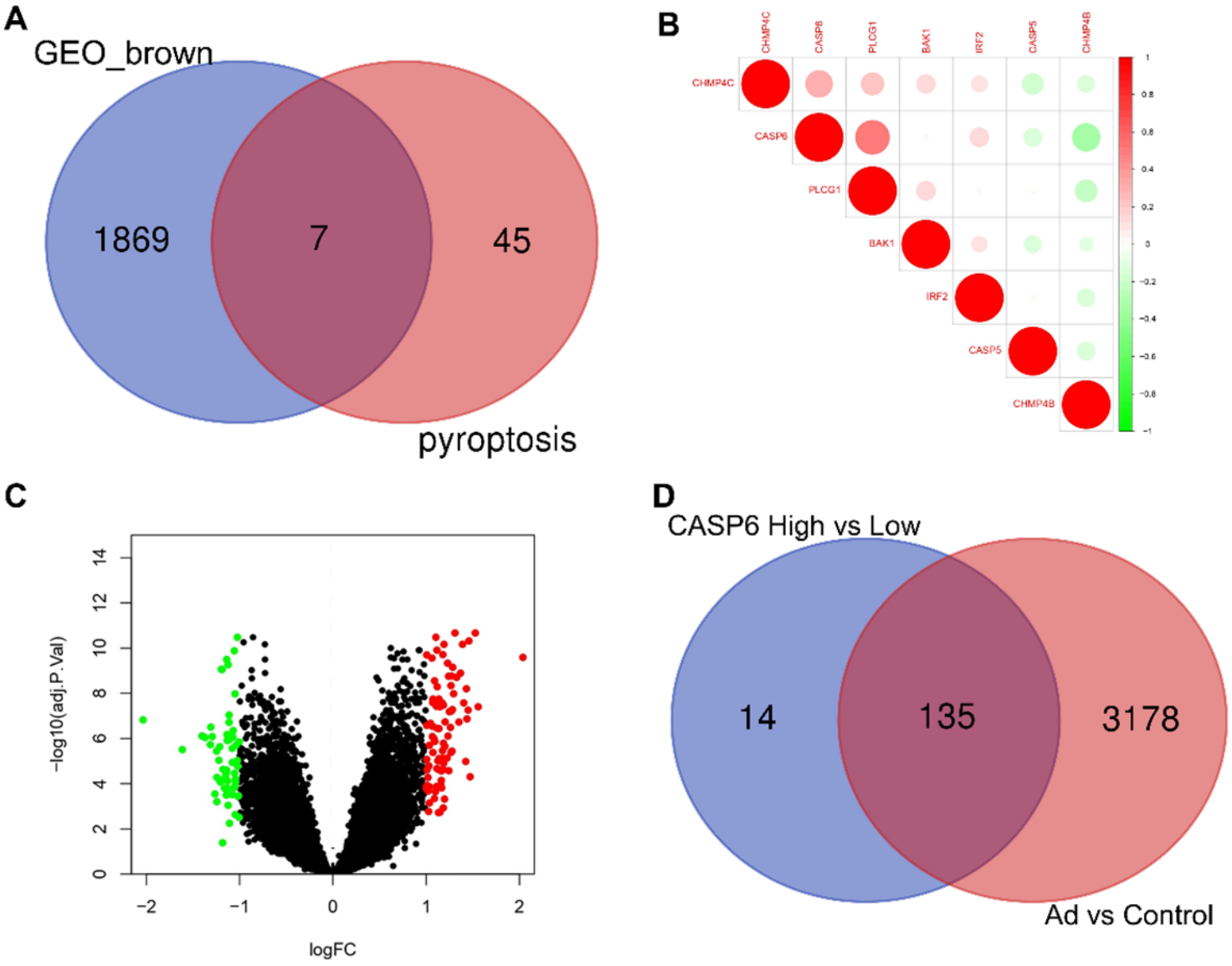

Figure 5

Intersection results of DEGs in brown module and pyroptosis-related genes. (**A**) Venn diagram of DEGs in the brown module and pyroptosis-related genes. (**B**) Correlations between seven overlapping pyroptosis-related genes. (**C**) Volcano plot of CASP6-high VS CASP6-low, red represents up-regulated genes, green represents down-regulated genes, and black represents insignificantly differentially expressed genes. (**D**) Venn diagram of DEGs from AD VS control and CASP6-high VS CASP6-low.

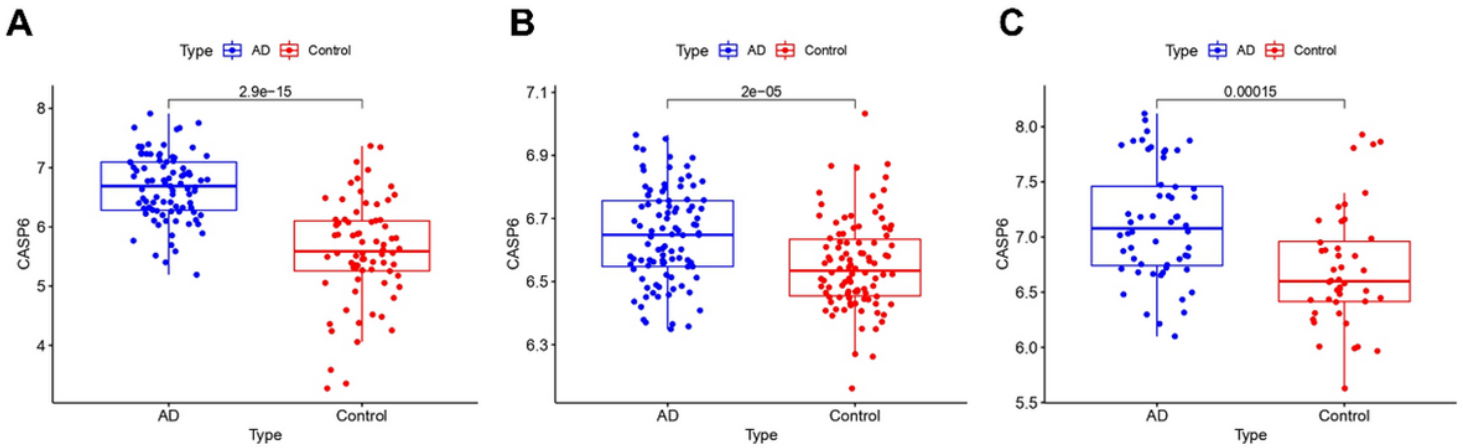

Figure 6

Identification and verification of differential expression of CASP6 in AD VS control. CASP6 is up-regulated in AD compared to controls in GSE5281 (**A**), GSE122063 (**B**), and GSE132903 (**C**).

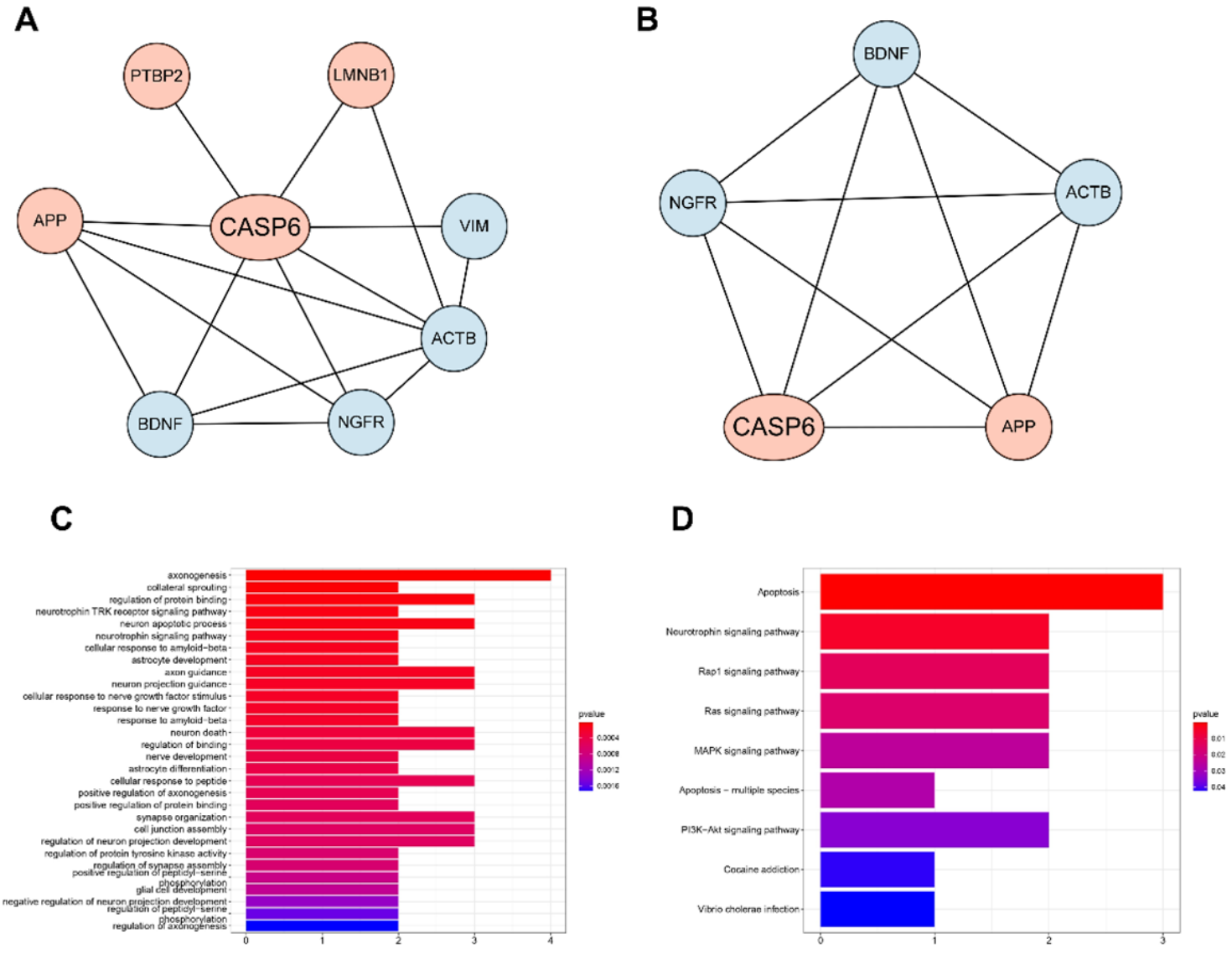

Figure 7

Interaction and functional enrichment analysis of CASP6 and seven hub genes. (**A**) protein-protein interaction (PPI) networks of CASP6 and seven hub genes, red represents up-regulated genes and blue represents down-regulated genes. (**B**) The most significant module from the previous PPI network. (**C**) Bar chart of enriched GO annotations for CASP6 and seven hub genes, ordered by P value. (**D**) Bar chart of enriched KEGG pathways for CASP6 and seven hub genes, ordered by P value.

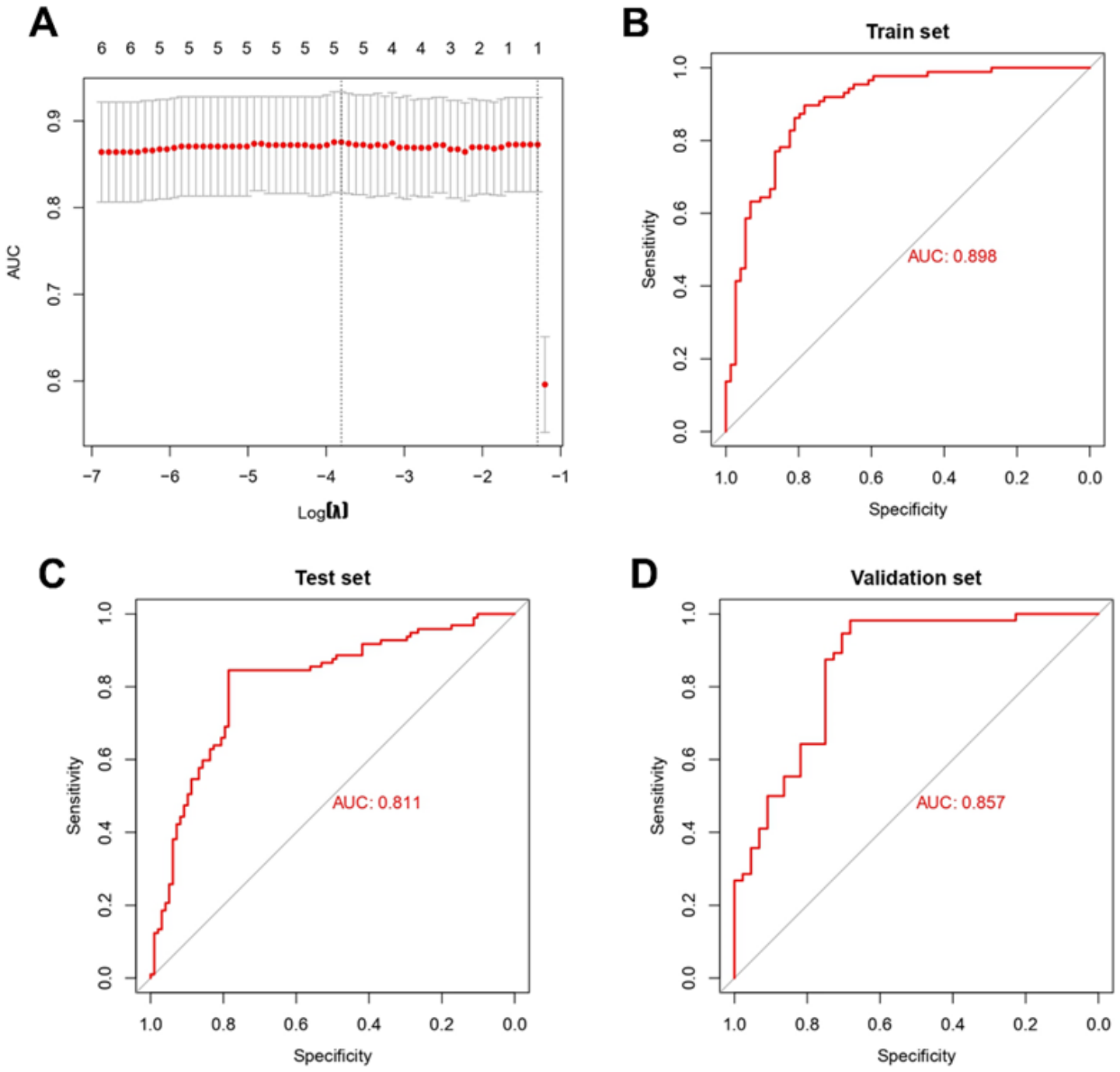

Figure 8

Construction of a key-gene-based LASSO model for AD.(**A**) LASSO regression of the seven key genes. (**B**) ROC curve of train set (GSE5281). (**C**) ROC curve of test set (GSE132903). (**D**) ROC curve of validation set (GSE122063).